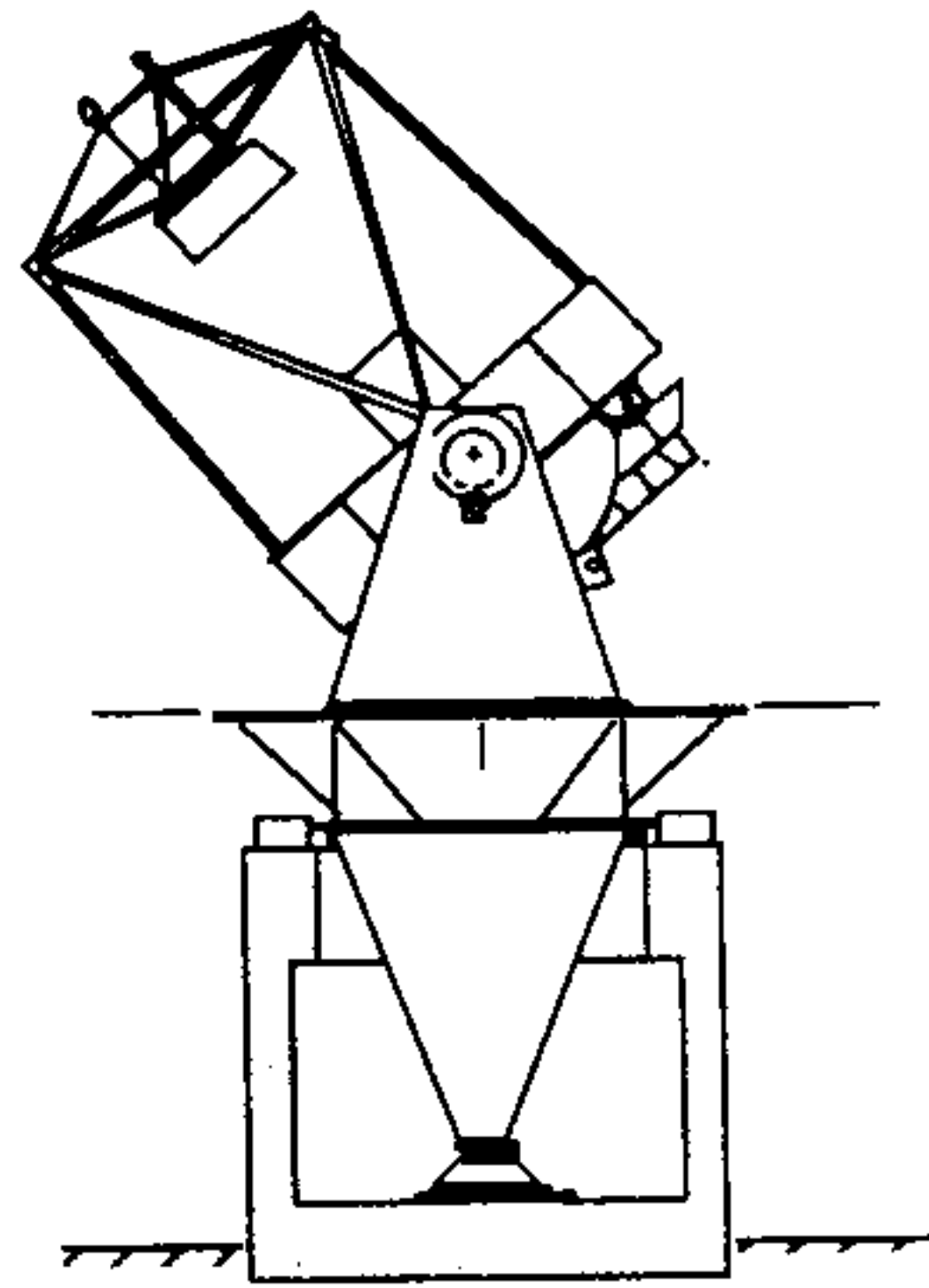


WISCONSIN
INDIANA
YALE
NOAO



3.5 METER TELESCOPE

**Azimuth Bearing Study
for the
WIYN 3.5 Meter Telescope**

WODC 02-06-01

5/22/91

1. Introduction..... 1
2. Test setup..... 2
3. Sensor Calibration..... 3
4. Results..... 3
5. Conclusions..... 5
6. Acknowledgements..... 5

1. Introduction

The WIYN 3.5-meter telescope will use Alt-Az design similar to the Astronomical Research Corporation (ARC) 3.5-meter telescope (see System Definition & Configuration, WODC 01-01). The pointing and tracking accuracy of the telescope will be affected by run-out and jitter in the bearings that support and define the azimuth axis. Of particular concern is the non-repeatable run-out that will be uncorrectable by the control system.

Surprisingly, bearing manufacturers are of little help in specifying the non-repeating characteristics of their bearings. Part of the problem is that the type of service these bearing encounter in a telescope greatly differs from their more common use in, for example, rolling mills. In the telescope, the main bearing rarely rotates more than two revolutions in one direction and then at very slow speeds.

During the preliminary design of the telescope mount, a spherical roller bearing was tentatively chosen for the lower azimuth thrust bearing. This type of bearing has the advantages of high load capacity and self-aligning properties. A possible disadvantage of these bearings is that they may not be as accurate as ball bearings because of the greater difficulty in making the rollers.

The ARC lower azimuth bearing is an SKF 29364E spherical roller bearing with a 320 mm inside diameter. WIYN decided to increase the clearance through the bearing to provide extra space for cables and has selected an SKF 29292 spherical roller bearing with a 460 mm ID. The roller and race cross section of the ARC bearing is slightly larger than WIYN (90 mm W. x 109 H. versus 80 mm W. x 95 mm H.) and the ARC bearing has a larger dynamic load capacity (2.9M N. versus 2.1M N.) but otherwise the bearings are similar. It was felt that a measurement of the run-out of the lower azimuth bearing on the ARC telescope would show whether this type of bearing is suitable for WIYN.

The upper end of the azimuth axis is defined by four rollers arranged in a square that roll on the outside cylindrical surface of the azimuth drive disk that is part of the fork assembly. The 140" diameter of the disk is the same for ARC and WIYN. Two diametrically opposed rollers are driven while the other two are idlers. Bearing types for WIYN's rollers haven't been selected at this time.

The support frame that attaches to the top of the pier and on which the rollers mount has been redesigned for WIYN to make it more stiff. The ARC support frame is a ring beam that carries some of the side loads of the telescope in bending. WIYN has replaced the ring beam with a square frame with all members acting in tension. Despite the differences in design, run-out measurements of the azimuth disk should provide WIYN data on the smoothness and out-of-roundness that can be achieved in the azimuth disk as well as baseline data for the roller stiffness.

The tests reported below involved a collaboration with Walt Siegmund and the staff and management of Apache Point Observatory.

2. Test setup

The pointing sensitivity of the WIYN telescope to a lateral displacement of the azimuth axis at the centers of the supports is 0.053 arcseconds/micron (one end fixed). The tracking and offsetting specifications are typically 0.1 arcsecond which requires a measuring accuracy of 1 micron or better for the run-out. A pair of Electro Corp. Model PA12D43 proximity sensors (MMTO #4 and #5) were borrowed from the Multiple Mirror Telescope Observatory for measuring the run-out. The PA12D43 is a non-contacting sensor that measures its distance from a conducting surface by setting up an rf field and measuring the power lost to eddy currents in the piece under test. The probe tip is 0.312" diameter and generates a sensing field of about 3/8" diameter at a working distance of about 1/8". The sensor includes signal processing electronics that outputs the separation as a voltage.

In the first set of tests on the lower azimuth bearing, the two sensors were mounted 180° apart on the fixed pedestal supporting the fork (Figure 1). A pair of gooseneck magnetic bases were used to secure the probes to the pedestal (Figure 2). Checks were made to see that the bases did not creep with time. The pair of sensors were used to separate out the effects of run-out from changes of diameter due to out-of-round surfaces.

The outer and inner surfaces of the bearing itself was not available for test and so a machined surface just above the bearing on the rotating fork was used. Any run-out between the bearing journal and this surface will show up in the test results. Although machined, the measured surface was not intended to be used for this purpose and the surface finish was only "fair". The diameter of the measured surface was 21.2".

The outputs of the proximity sensors were digitized with a Strawberry Tree Model ACM2-12 8-channel A/D board running in a Mac II computer. The ACM2-12 has 12-bit resolution and autoranging. Two channels were connected to the output of the two sensors. A third channel sampled the output of the Sony Magnesensor that provides absolute fiducial marks for the azimuth rotation. This channel was later used to synchronize successive scans. Strawberry Tree's QuickLogMac software was used for logging the data.

The test procedure was to start the axis rotating at a fixed rate and continuously sample the outputs of the sensors at a fixed rate set by the software. We relied on the rotation rate stability of the drives to provide the positional accuracy of the measurement between fiducial marks.

In the second set of tests, the probes were moved to the upper azimuth disk and mounted on the frame supporting the rollers. In retrospect, it would have been better to mount them directly on the pier to measure relative movement of the telescope relative to the pier and remove a source of uncertainty.

Various sample rates and axis scan rates were tried during the tests. For the results reported here, the sample rate was 5/second and the scan rate was 1°/second. This provides 1800 sample points per revolution with adjacent points separated by 0.244" on the 140" diameter disk and 0.036" at the lower azimuth bearing. The corresponding angular resolution is about $(140" \times \text{PI}) / (2 * 0.375") = 590$ cycles per revolution on the azimuth disk and $(21.2" \times \text{PI}) / (2 * 0.375") = 89$ cycles per revolution on the azimuth bearing.

The data was reduced and graphed using MicroSoft Excel running on the Mac. Sums and differences of the data pairs were computed at each angle to obtain the change in diameter and run-out of the measured surface as a function of rotation angle. The run-out is half the measured difference. As plotted, depressions in the surface show up as peaks in the diameter data.

3. Sensor Calibration

Before going to APO, the gain of the sensors were calibrated by mounting each sensor on the bed of a milling machine and moving it relative to a fixed reference plate mounted on the head. The voltage from the sensor was recorded as a function of carriage position. The digital readouts of the mill are accurate to 0.0001". A multimeter with 3-1/2 digit resolution was available for the tests of sensor #4 for a resolution of 2.5 micron. A 5-1/2 digit multimeter was used for tests on sensor #5. Tables 1-2 and the corresponding Figures 3-4 show the calibration results.

To test long-term stability, a jig was made to hold the sensor in a fixed position relative to the reference surface. Measurements were taken after a 1 hour warm-up period. The measured voltage drift under constant temperature was:

Sensor #4:	1.1 mv/hr
Sensor #5:	0.4 mv/hr

which correspond to separation measurement errors of 0.3 and 0.1 micron/hr respectively.

At APO the test was repeated with the sensors mounted on the azimuth pedestal in the configuration used to measure the run-out of the fork. The Mac was used to record the data. Figure 5 shows the sensor outputs after a 1 hour warm-up. Drift is less than 0.1 micron/hr for both sensors.

4. Results

Figure 6 shows the computed diameter variation for two scans (numbers 32 & 41) taken on successive days. During the intervening night, the telescope was exercised heavily while performing a supernova search. After adjusting for a slight overnight DC drift in the sensors, the plotted data for the two scans are indistinguishable. Surface irregularities and a small (~40 microns) amount of out-of-round is apparent.

Figure 7 shows the repeatability of the measurement from one day to the next. The RMS scatter of the points is 0.92 microns and the digitization of the A/D is apparent. A clear, systematic change in the run-out at the 2 micron p-v level in the range 150° to 270° is apparent. The sharp peaks at 90°, 160°, and, to a lesser extent, at 270° and 350° result from imperfect phase matching of the two scans in the vicinity of sharp features in figure 6. Much of the rest of the scatter in the plot may also arise from phase jitter in the measurements and 0.92 microns represents an upper limit to the diameter repeatability. The feature from 170° to 270° persisted despite attempts to adjust the relative phase of the two scans in fractional sample-time steps and is probably real.

The real parameter of interest in these tests is the bearing run-out since it is directly related to the telescope pointing. Figure 8 shows the

measured run-out for the two scans. The RMS variation is 16.2 microns. The sharp prominent spikes are caused by surface features (dings and holes adjacent to the scan path) that don't affect pointing. Unfortunately there is no way to separate the bearing run-out from run-out of the measured surface with respect to the bearing or to remove the affects of surface roughness.

Instead we look at the repeatability of the run-out (figure 9) to find the portion of the error that can't be removed with the telescope pointing map. The RMS value of the non-repeatable run-out is 0.61 microns which corresponds to an 0.03 arcsecond RMS pointing error on WIYN. The measured non-repeatable run-out includes the effects of phase jitter and 0.03 represents an upper limit to the actual pointing error that would show up during observing due to azimuth bearing run-out.

Measurements of the azimuth disk were taken off the surface used for encoding the axis. Two scans, 21 & 22, were taken one after the other on the same day. Figure 10 shows the diameter change of the disk with rotation angle. The disk is out-of-round by 0.0025%. In addition, several dents show up in the data. A pair of these may be associated with joints where the two halves of the disk were welded together during fabrication (Siegmond, private communication). It isn't clear whether an actual depression occurs at those locations or whether the spike is caused by different material properties in the area of the weld. There appears to be a high frequency periodic component in the data which will be analyzed in a later report.

Figure 11 shows the repeatability of the disk diameter measurements. The RMS variation is 2.6 microns. The larger scatter in the disk repeatability measurements compared to the azimuth bearing results may be a result of phase jitter between scans coupled with the higher "bandwidth" of the disk measurements detecting high frequency ripple in the surface.

The 370 micron p-v run-out of the azimuth disk provided the greatest surprise of the tests. The direction of the error is in-line with one of the fork tines. A large (approximately 2000#) spectrograph was mounted at the Nasmyth port during the tests and may have unbalanced the telescope. Adding approximately 350 pounds to the opposite tine brought the azimuth disk back 10 microns, not enough to explain the 370 micron run-out. Time didn't permit further tests to identify the source of the error.

There is a significant amount of high frequency ripple in the run-out of the azimuth disk with amplitudes of 5 microns and more. Figure 13 shows an expanded section of the run-out data which shows this. This run-out will produce observable tracking errors if left uncorrected. Correcting the run-out with the pointing map would require an excessively fine mesh and lengthy calibration procedures.

The repeatability of the run-out in the azimuth disk, figure 14, is 3.7 microns RMS corresponding to 0.20 arcseconds on the sky. While some fraction of this is measurement noise due to jitter, it is not clear that the high frequency components, even if repeatable, can be completely compensated in the pointing corrections.

5. Conclusions

The type of spherical roller bearing used for the lower azimuth bearing on the ARC telescope can meet the pointing and tracking specifications of WIYN with pointing corrections provided by the control system. Tests on the completed telescope will be required to determine the degree of meshing required in the pointing map. The design of the fork and lower bearing assembly should provide access to the bearing or a ground surface (0.5 micron RMS) concentric with the bearing journal to allow measurements to be made free of the high frequency surface ripple.

The pointing and tracking performance provided by the upper azimuth disk may be marginal for meeting the specifications for offsets and open-loop tracking. The cause of the large run-out needs to be identified and an effort should be made on WIYN to eliminate the high spatial frequency noise that will be difficult to remove with the control system.

6. Acknowledgements

This is to acknowledge the contributions of the following people to the project:

Walter Siegmund for his full collaboration in the project.

Charles Hull for his assistance in setting up and conducting the tests.

Apache Point Observatory for providing equipment and making time available on the 3.5-m telescope.

Multiple Mirror Telescope Observatory for the loan of the proximity sensors.

Roger Rupp for making the test jig and providing other assistance.

--Matt Johns, 5/21/91

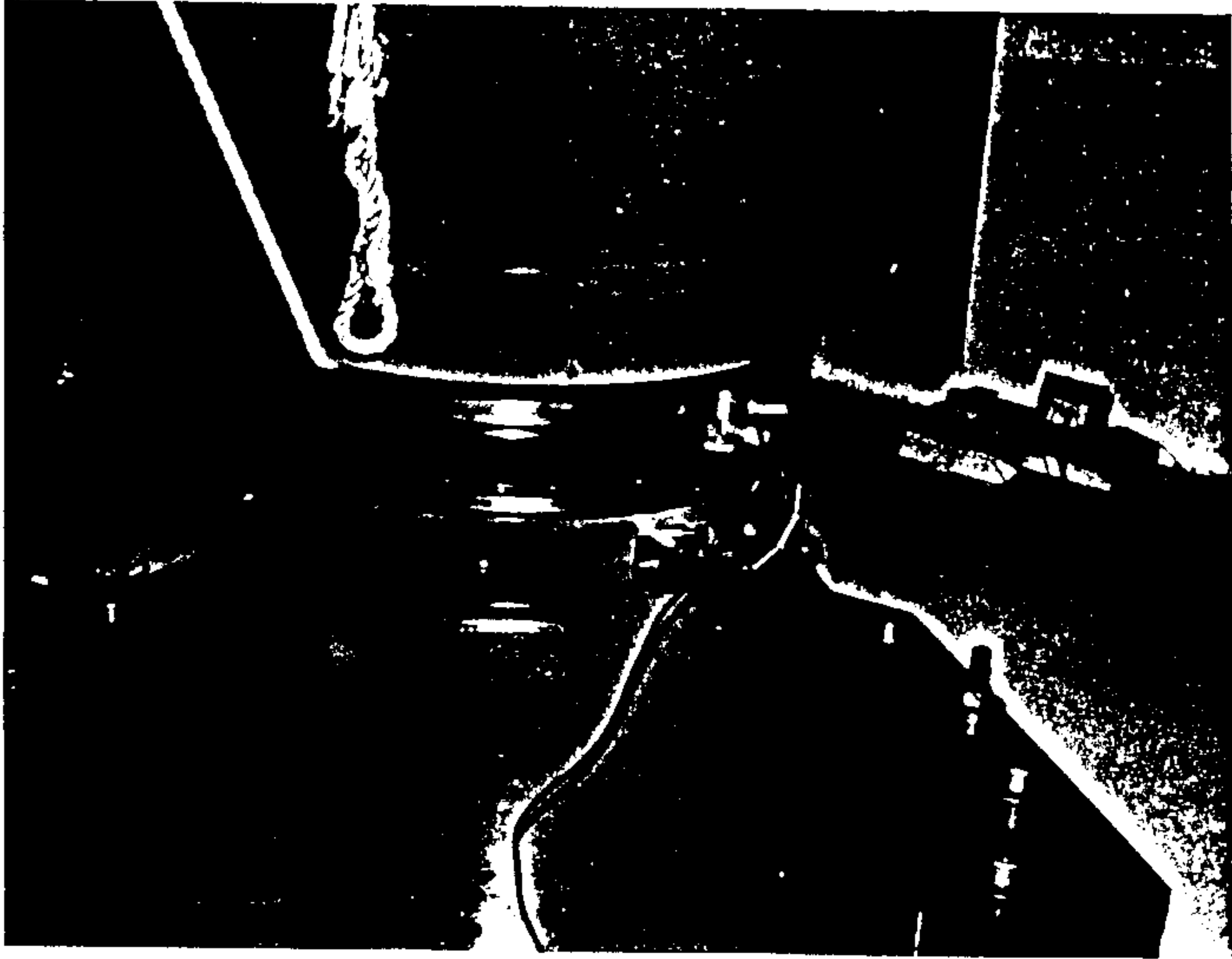


Figure1. Test set-up on ARC 3.5-m Telescope.

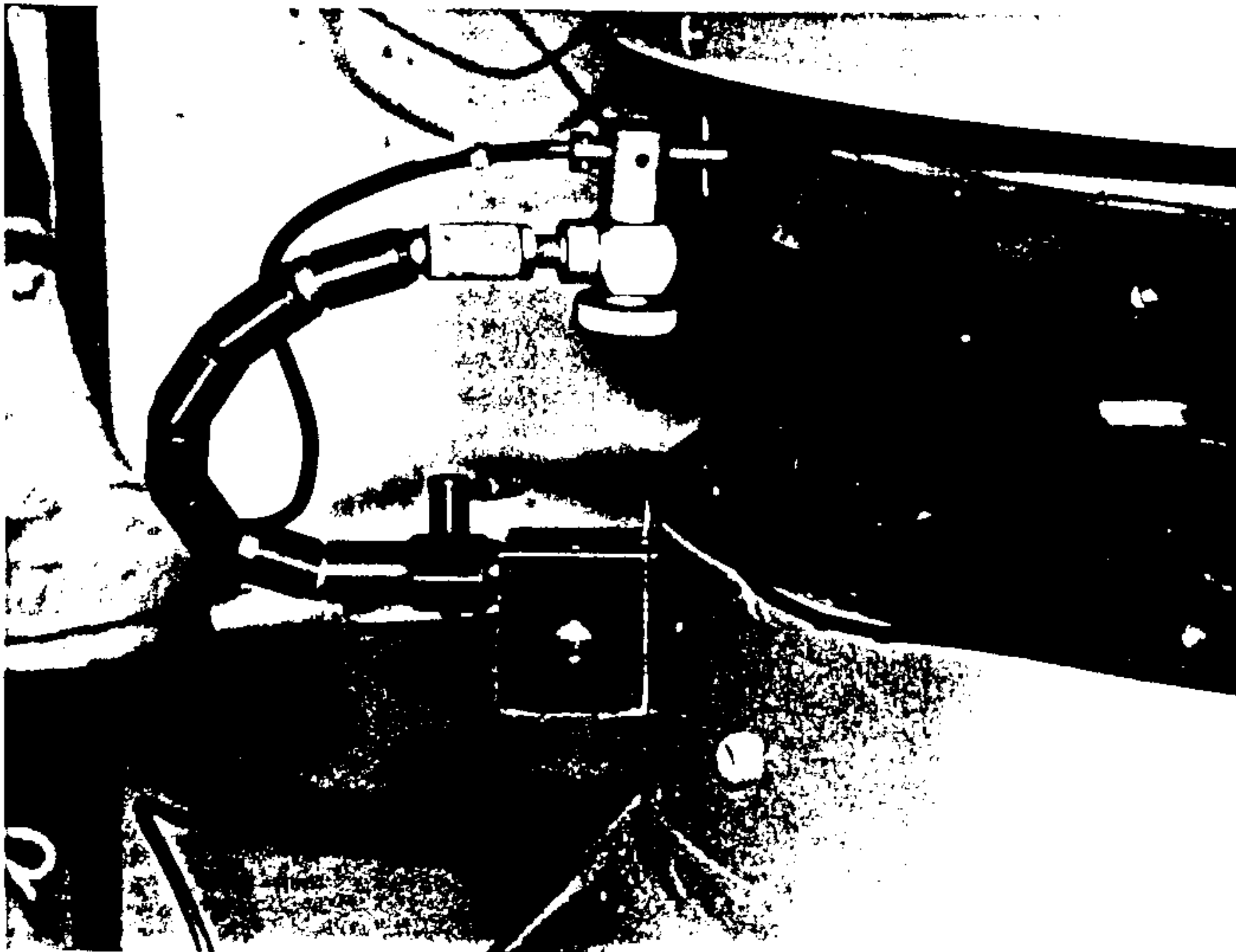


Figure 2. Close-up view of sensor mounting.

Table 1. Sensor #4 Calibration

Sensor calibration					
Type	Electro-Mike Inductive Proximity Sensor				
Model:	PA12D43				
Sensor #4	Full range	Center			
Scale:	-98.93	-100.00	volts/in.		
Offset:	14.06	14.25	volts		
RMS:	0.12	0.00	volts		
x (in.)	V (volts)	Full range ax+b	delta	Center ax + b	delta
0.0265	11.21	11.44	-0.23		
0.0405	10.00	10.06	-0.06		
0.0520	9.00	8.92	0.08		
0.0625	8.00	7.88	0.12	8.00	0.0000
0.0725	7.00	6.89	0.11	7.00	0.0000
0.0825	6.00	5.90	0.10	6.00	0.0000
0.0925	5.00	4.91	0.09	5.00	0.0000
0.1025	4.00	3.92	0.08	4.00	0.0000
0.1115	3.00	3.03	-0.03		
0.1210	2.00	2.09	-0.09		
0.1305	1.00	1.15	-0.15		

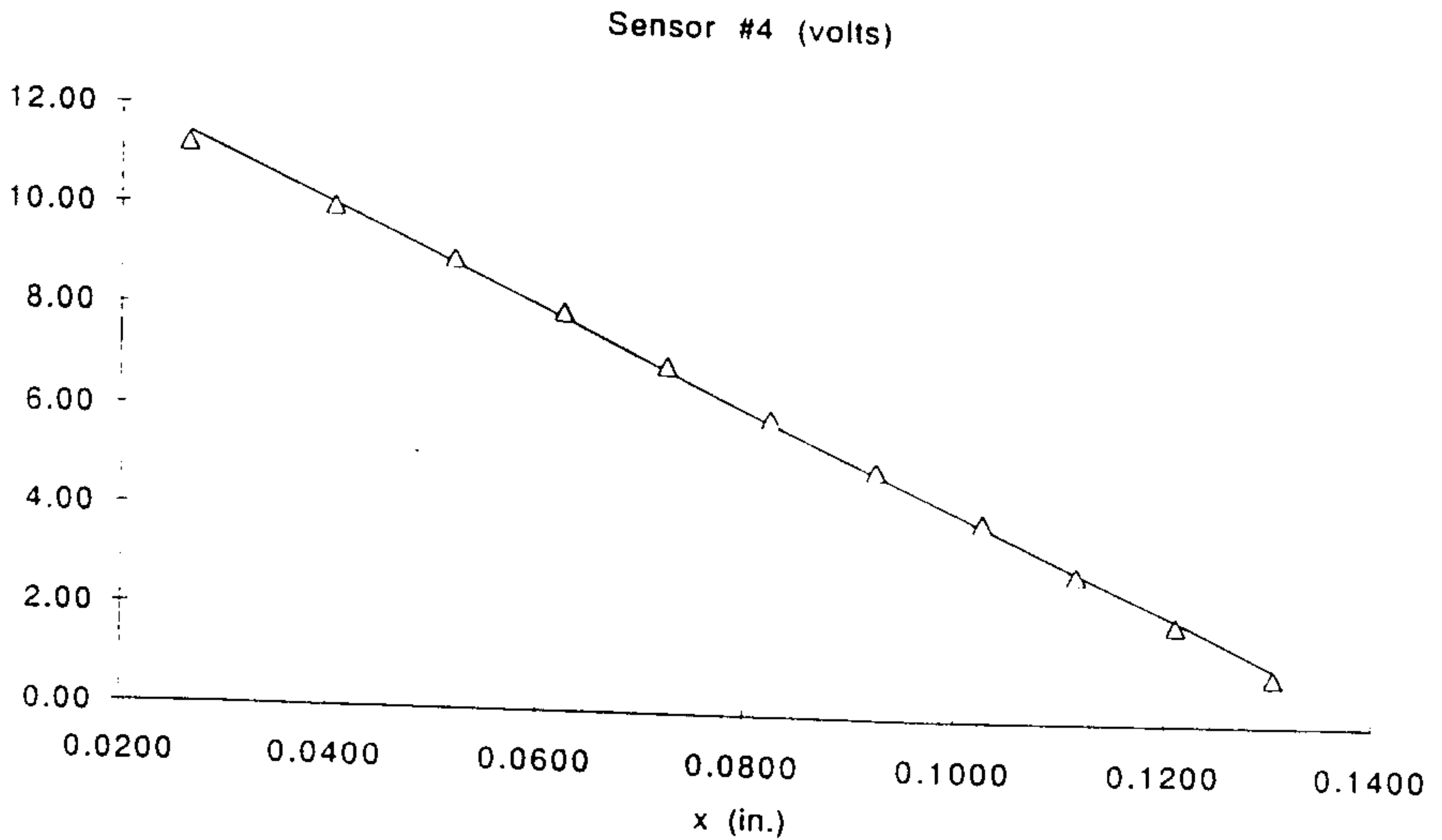


Figure 3. Sensor #4 linearity.

Table 2. Sensor #5 Calibration

Sensor calibration						
Type	Electro-Mike Inductive Proximity Sensor					
Model:	PA12D43					
Sensor #5						
	Full range	Center				
Scale:	-91.79	-92.26	volts/in.			
Offset:	12.15	12.33	volts			
RMS:	0.17	0.04	volts			
		Full range		Center		
x (in.)	V (volts)	ax+b	delta	ax + b	delta	
0.0200	10.0292	10.32	-0.29			
0.0300	9.2881	9.40	-0.11			
0.0400	8.5029	8.48	0.02			
0.0500	7.6780	7.56	0.12	7.72	-0.04188	
0.0600	6.8180	6.64	0.17	6.80	0.0207	
0.0700	5.9151	5.73	0.19	5.87	0.04038	
0.0800	4.9768	4.81	0.17	4.95	0.02466	
0.0900	3.9857	3.89	0.09	4.03	-0.04386	
0.1000	2.9987	2.97	0.03			
0.1100	1.9592	2.06	-0.10			
0.1200	0.8454	1.14	-0.29			

Sensor #5 (volts)

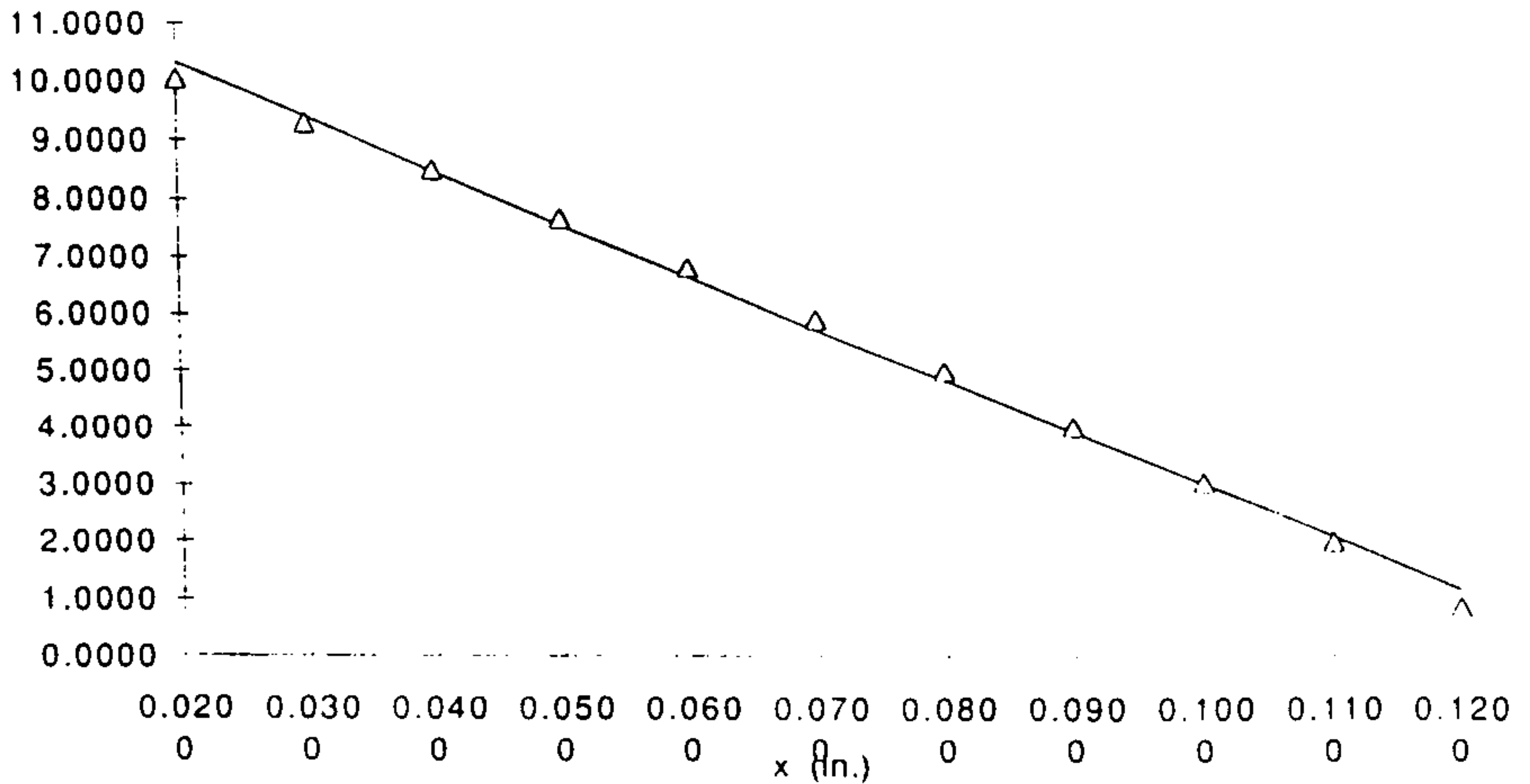


Figure 4. Sensor #5 linearity.

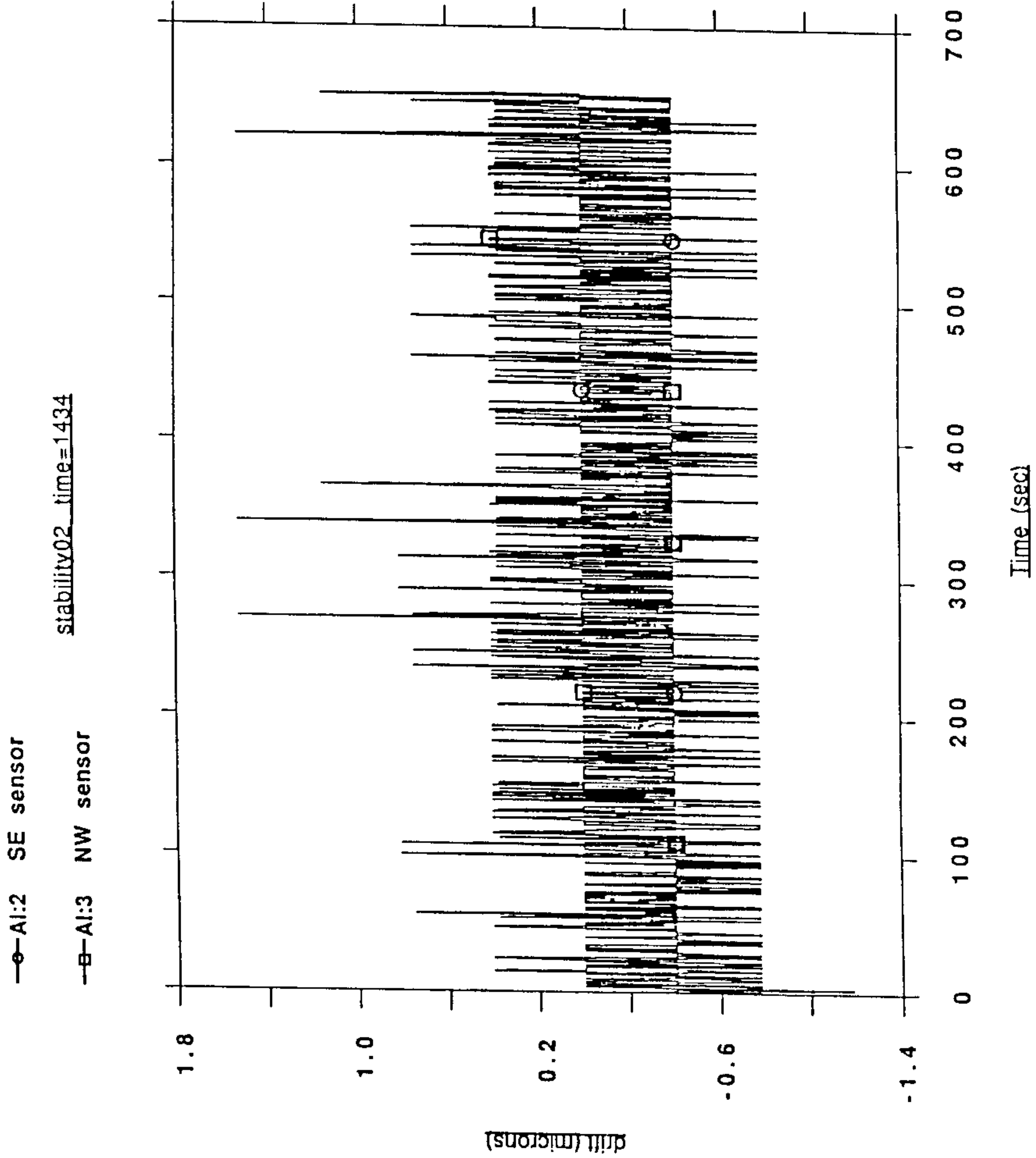


Figure 5. Sensor stability mounted on telescope.
 Circles = sensor #4. Squares = sensor #5.

Azimuth Bearing

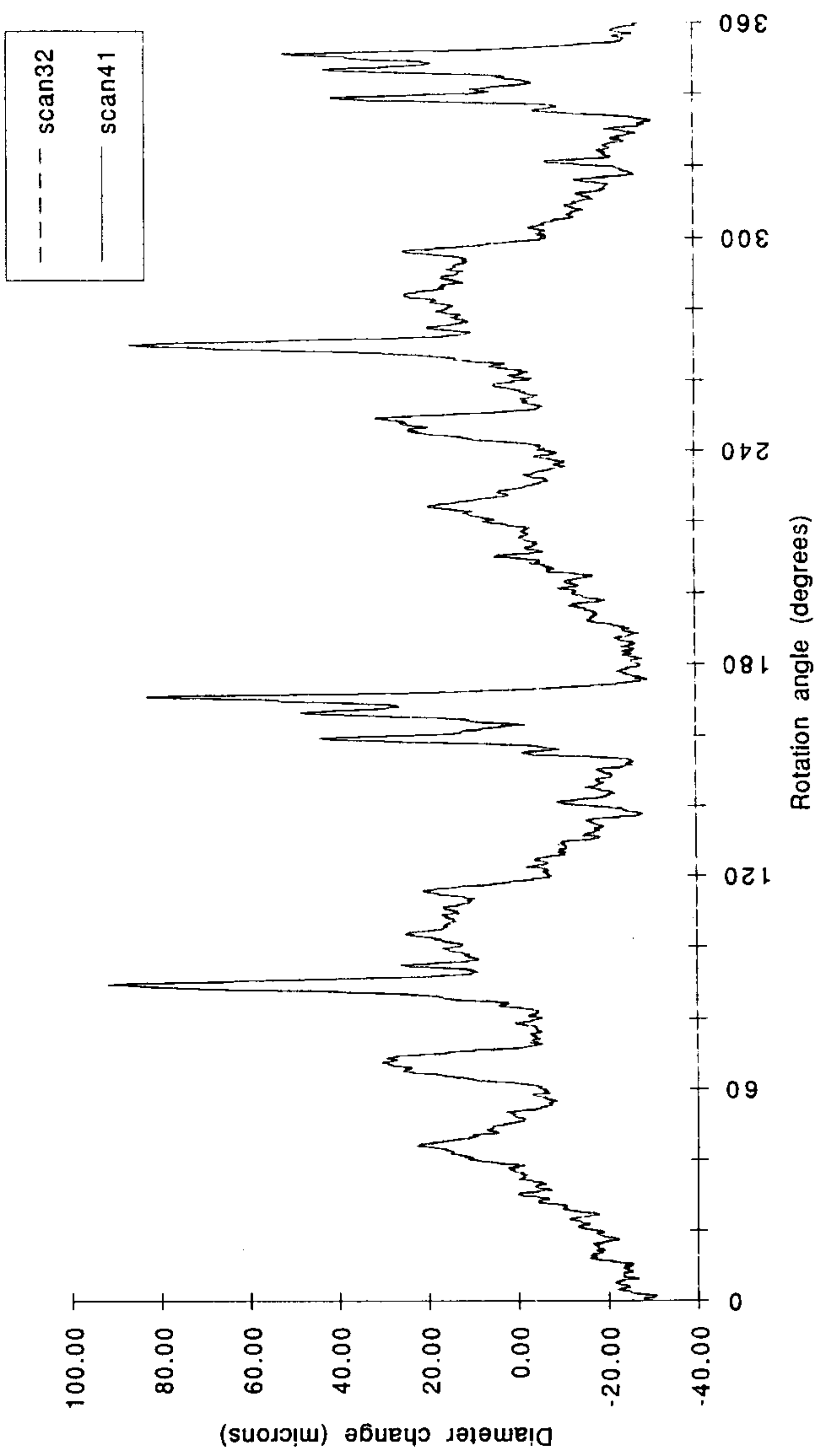


Figure 6

ARC Bearing Tests

Azimuth Bearing (Scans 32 & 41)

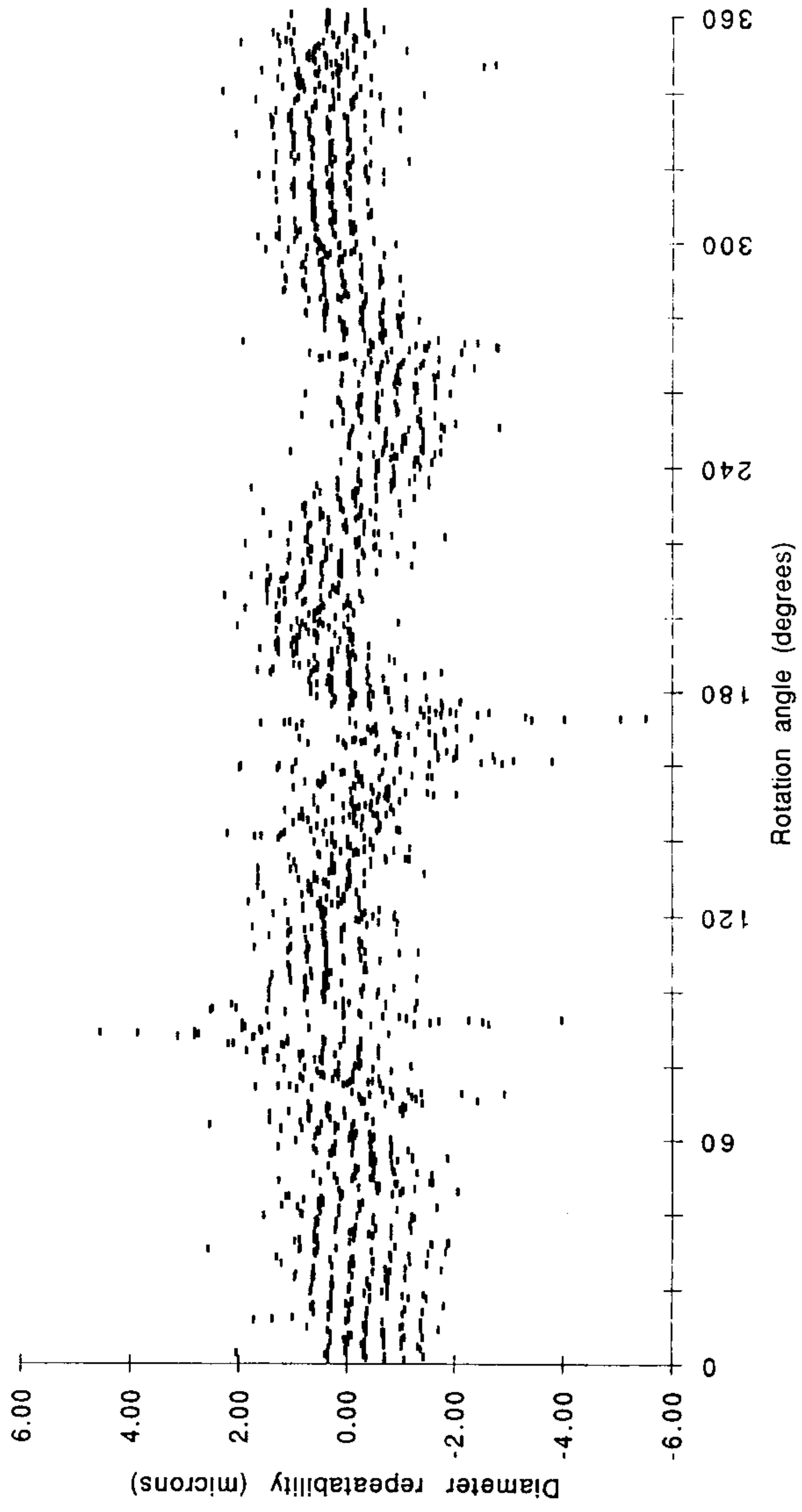


Figure 7

Azimuth Bearing

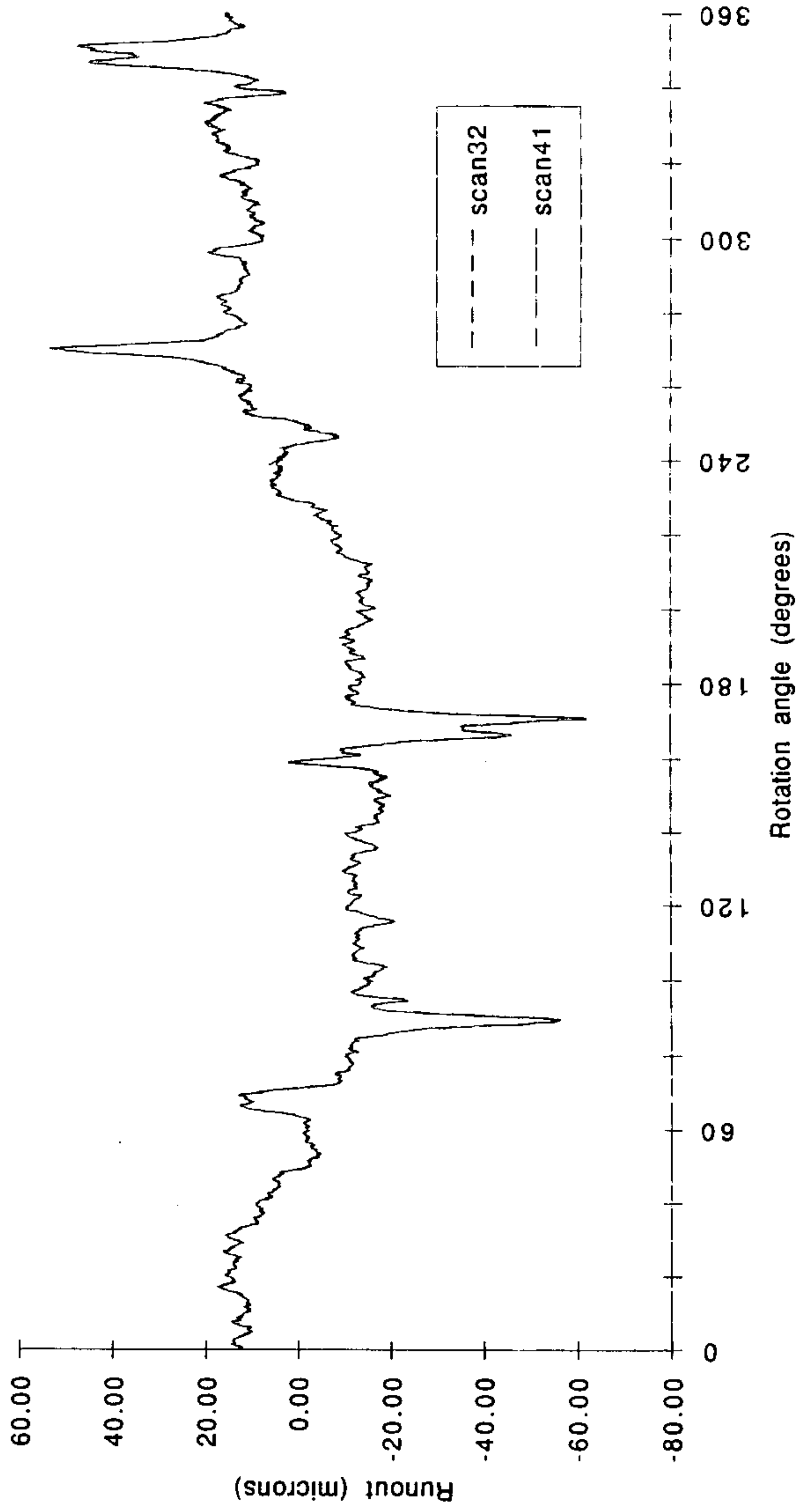


Figure 8

ARC Bearing Tests

Azimuth Bearing (Scans 32 & 41)

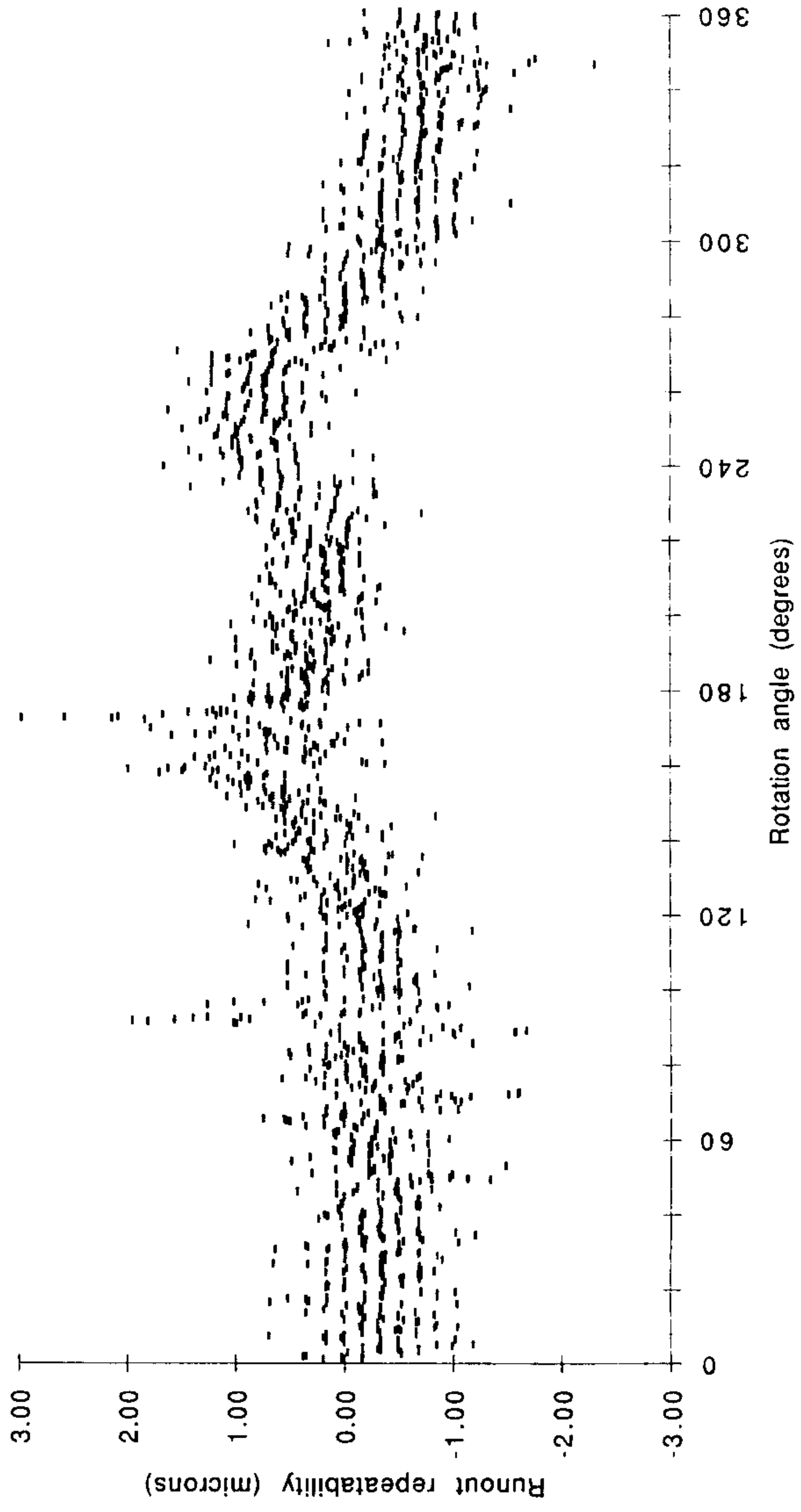


Figure 9

Azimuth Disk

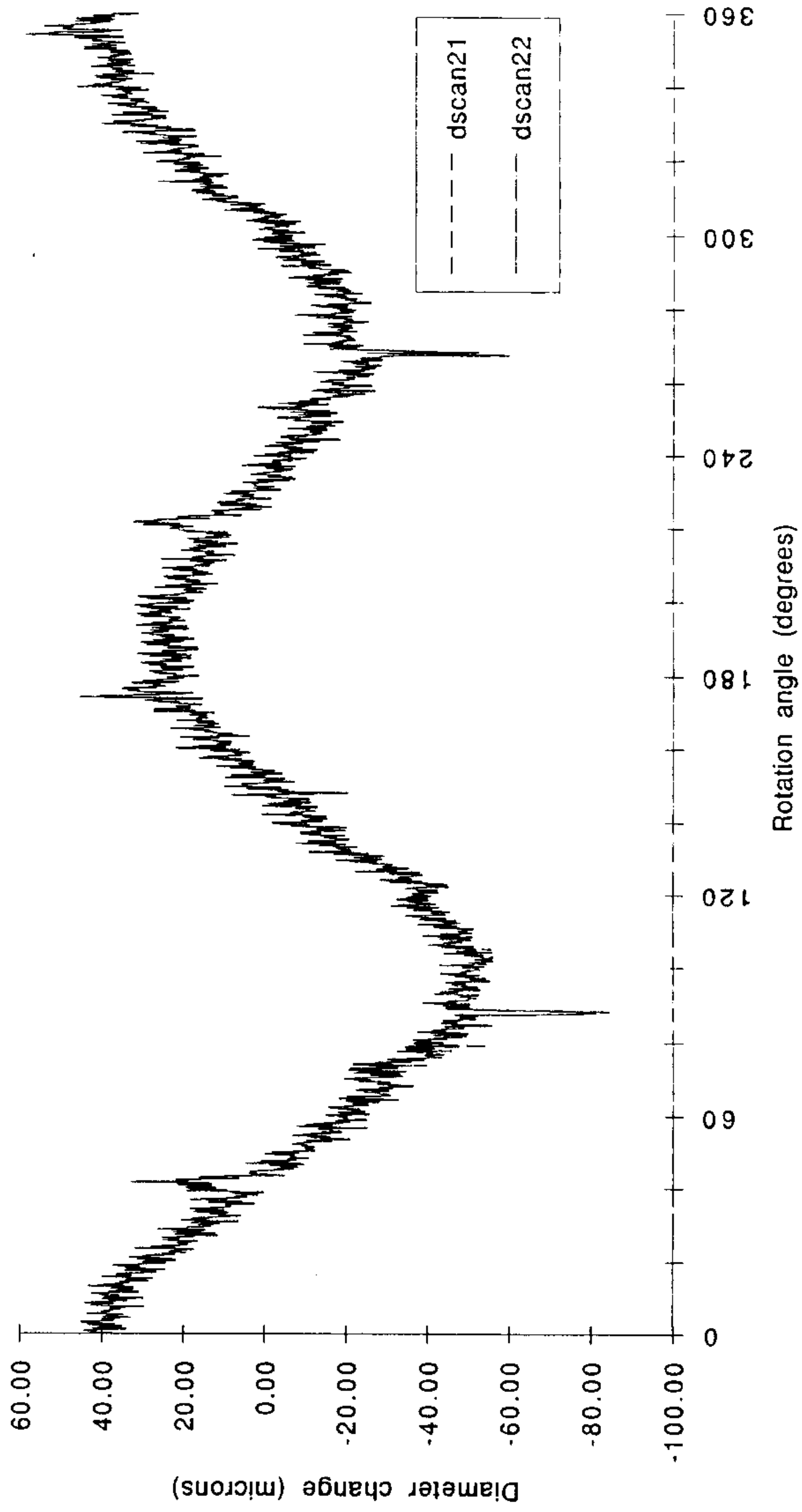


Figure 10

Azimuth Disk (Scans 21 & 22)

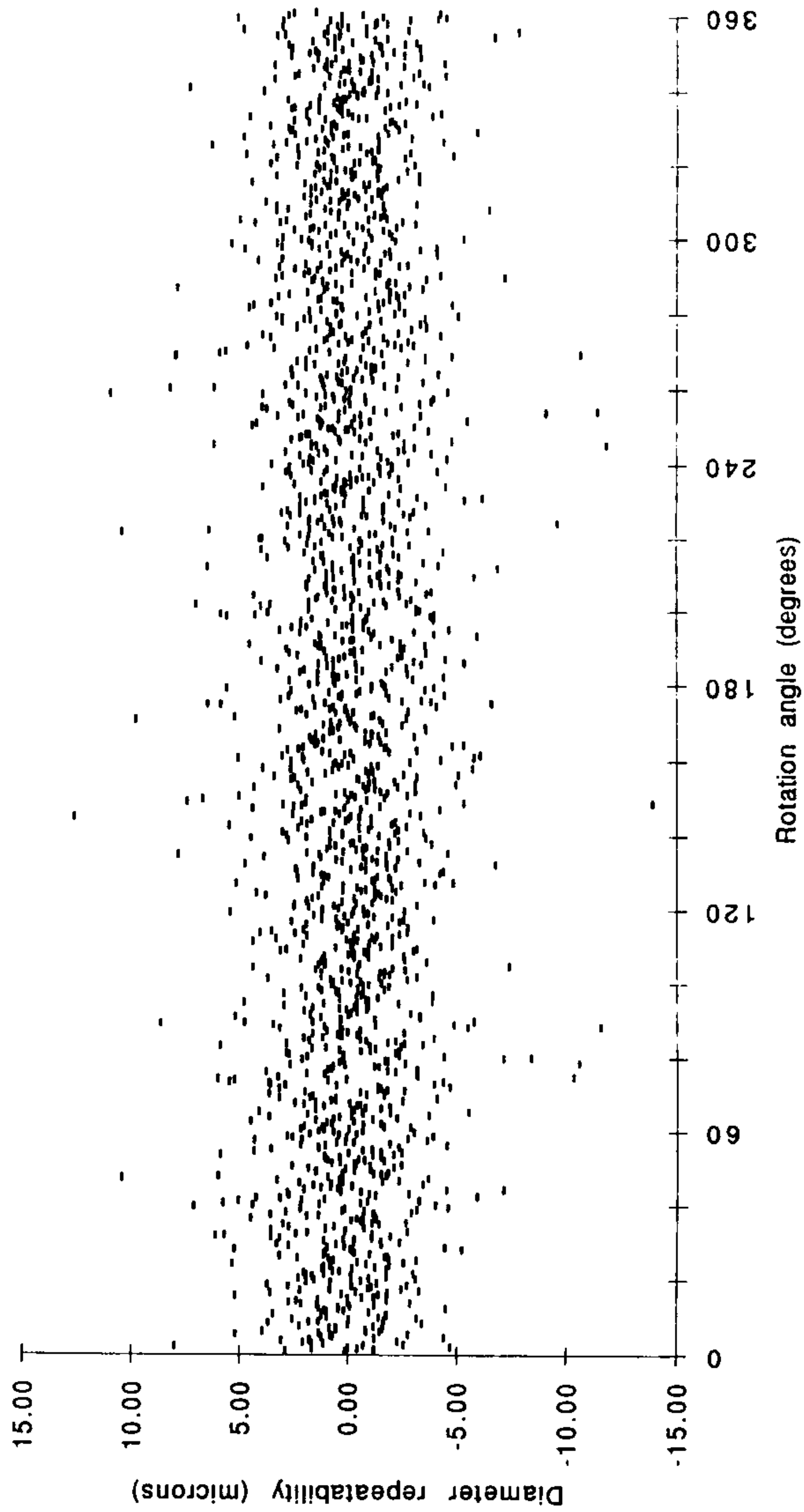


Figure 11

Azimuth Disk

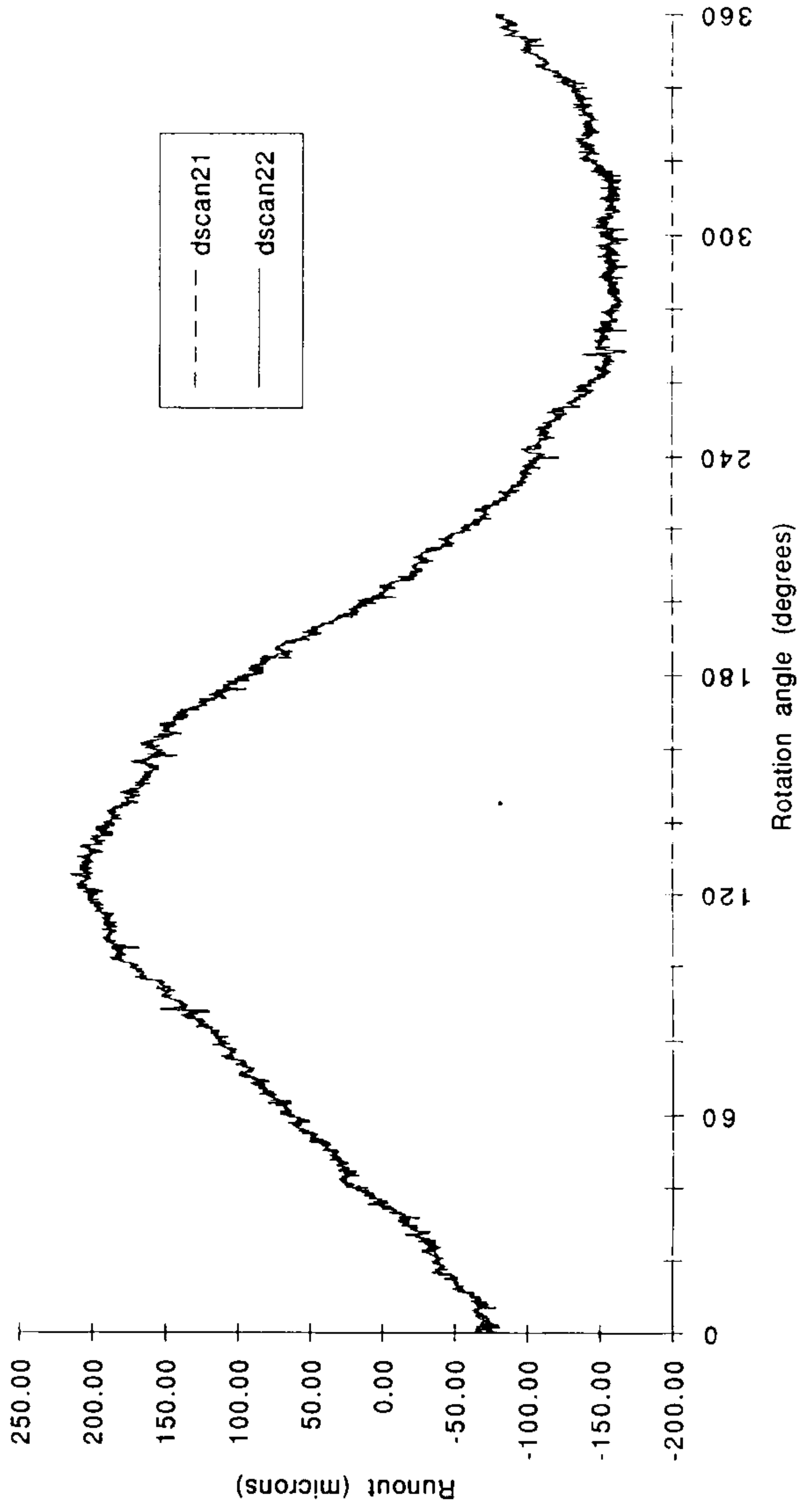


Figure 12

ARC Bearing Tests

Azimuth Disk

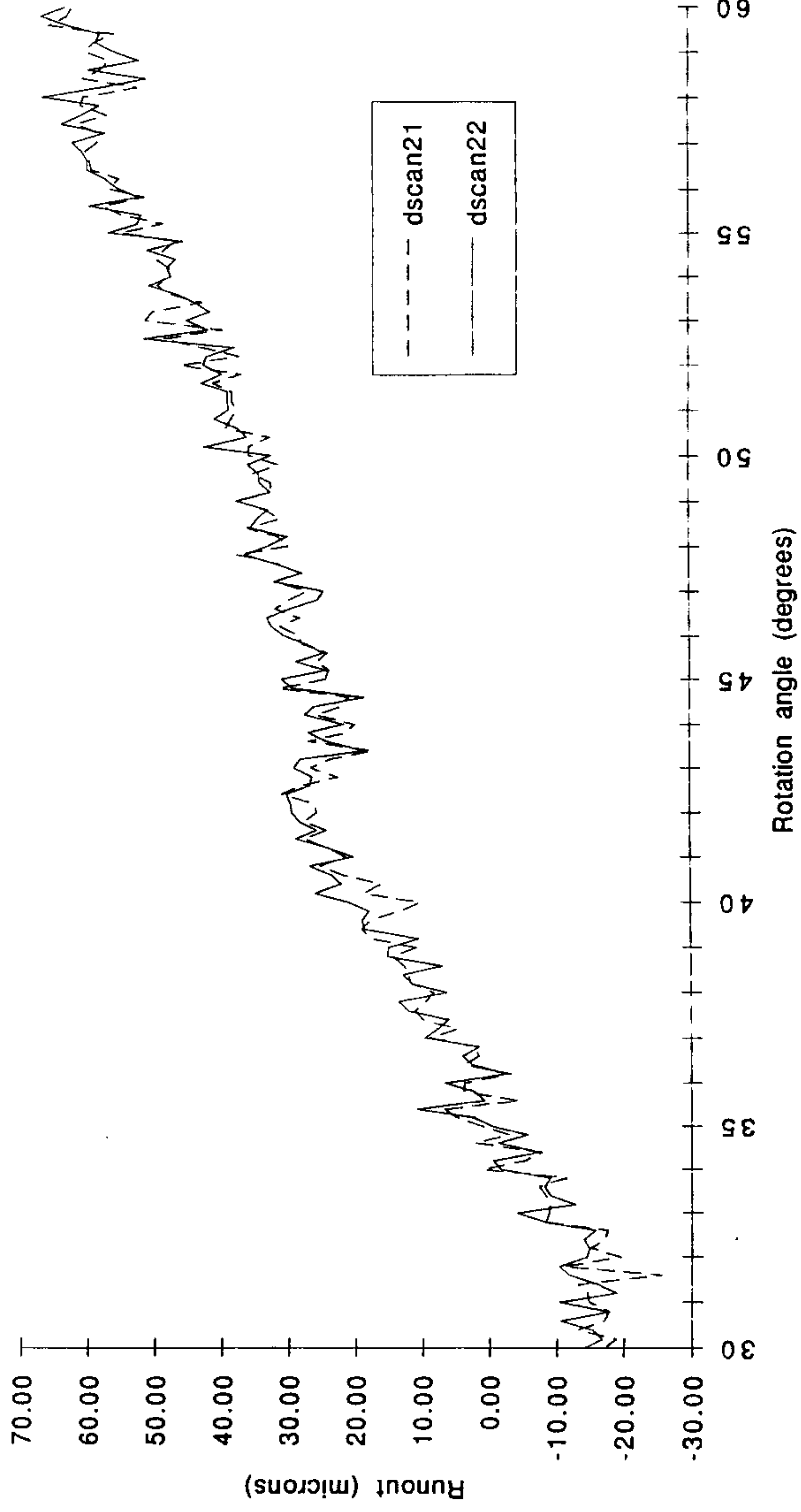


Figure 13

ARC Be. g Tests

Azimuth Disk (Scans 21 & 22)

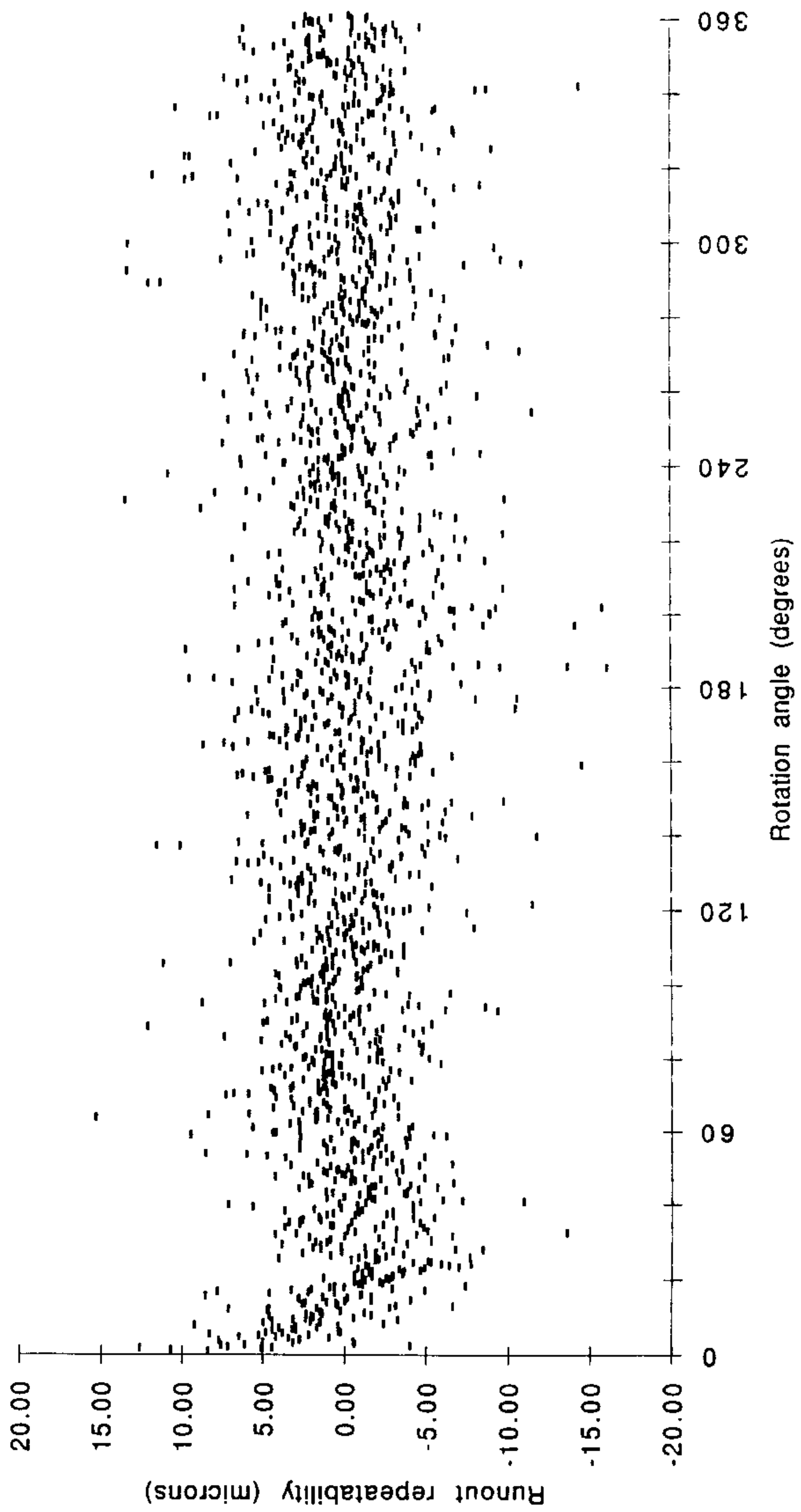


Figure 14